Compton process and two-phase medium

1. Introduction

Multi-phase medium is present in our every day experience. In most obvious cases the stratification is related to the medium content (ground/air transition, water/air transition), more subtle examples are clouds, rain droplets.

Apparently simpler are examples of two-phase medium of identical contect, for example of three forms of water

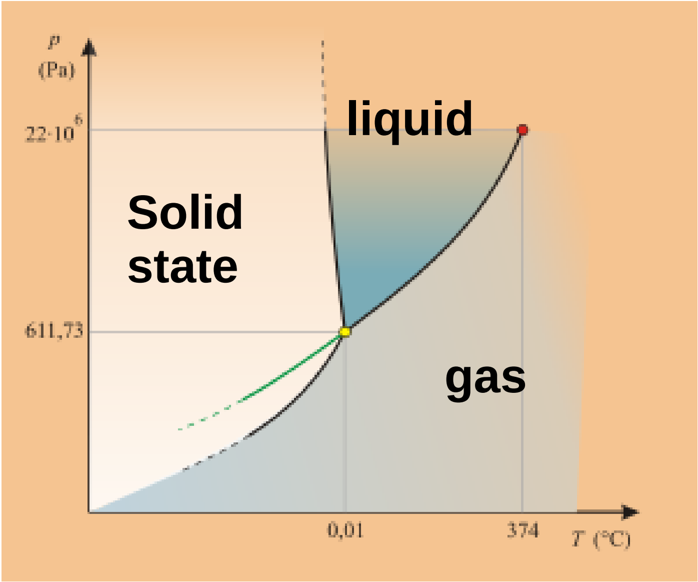

Triple point of water (wikipedia)

https://www.princeton.edu/news/2018/01/10/spotty-coverage-climate-models-underestimate-cooling-effect-daily-cloud-cycle

1. Introduction

Two-phases coexist under certain balance requirements, usually pressure balance is satisfied and the discontinuity corresponds to the change of the density, chemical composition, matter state (solid/liquid etc.).

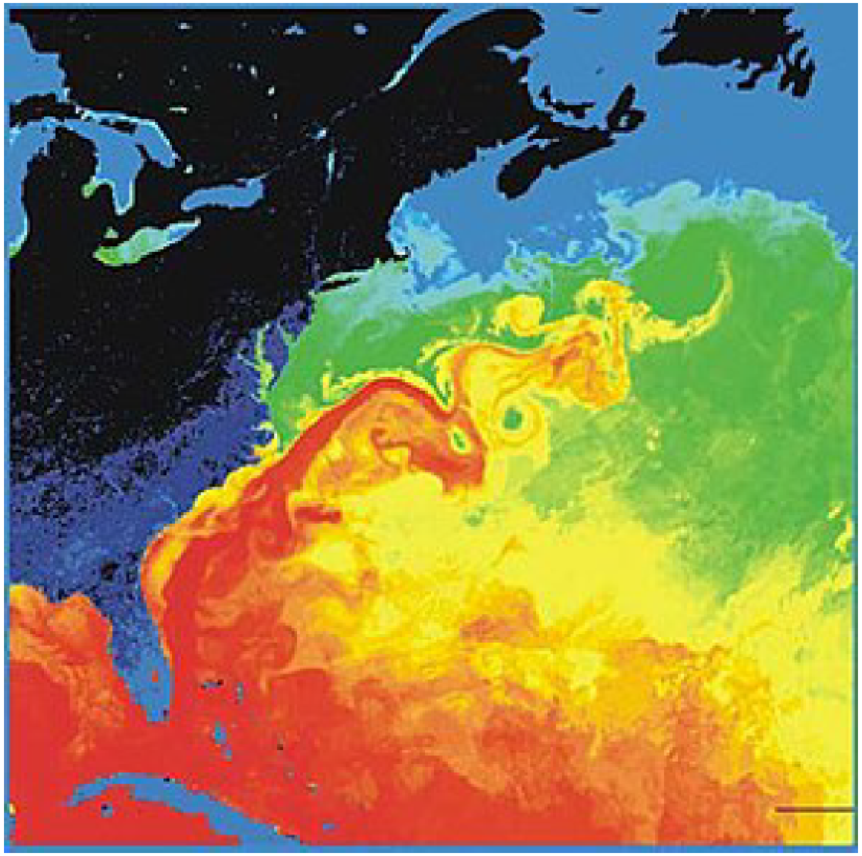

Temperatura powierzchni północno-zachodniego Atlantyku. Ameryka Północna ma kolor czarny i ciemnogranatowy, a Prąd Zatokowy – czerwony

From wikipedia (pl)

For example, Gulf Stream waters differs from the rest of Atlantic water with respect to the temperature and the salt content. The stream is relatively narrow (100 km wide) and shallow (depth of 800 m), and fast (up to km/h or equivalently 2.5 m/s).

In astronomy, multi-phase medium is everywhere, including accreting sources.

1. Introduction

One example of a two-phase medium in astronomy is the solar corona. The effective temperature of the Sun is 5777 K, while the temperature of the corona reaches over 10^6 K.

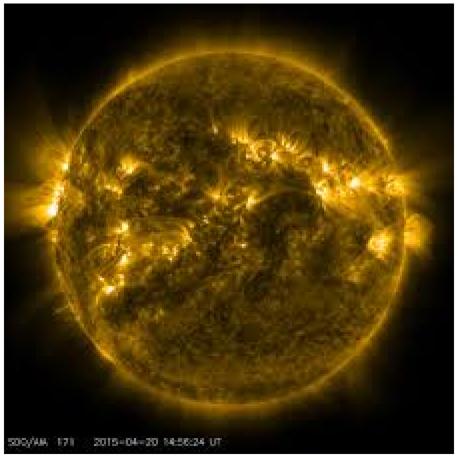

Sun from SDO (Solar Dynamic Observatory) in UV

In the Sun the amount of radiation clearly different from a black body emission is variable but always small.

A photo of the Sun – BBC radio

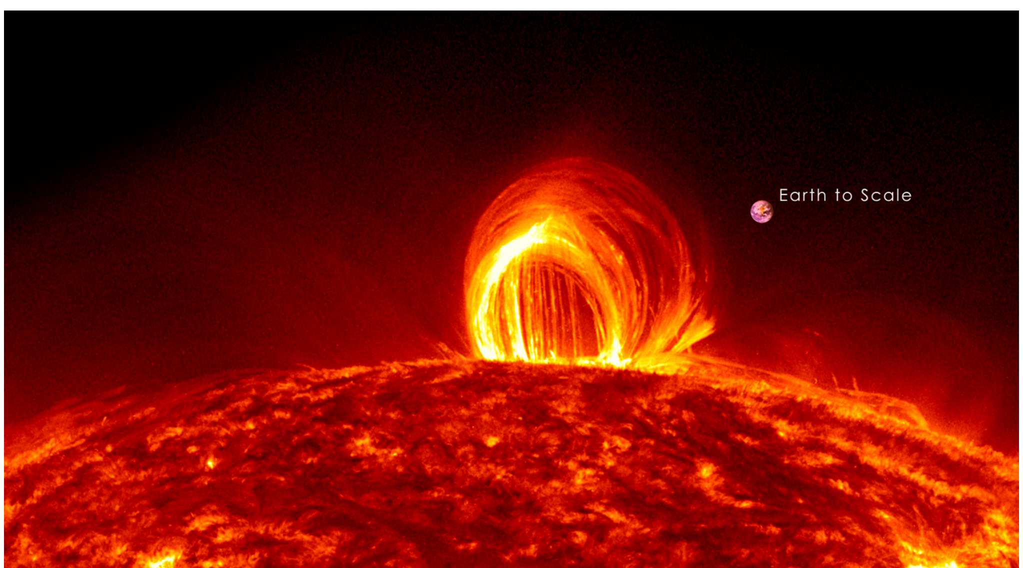

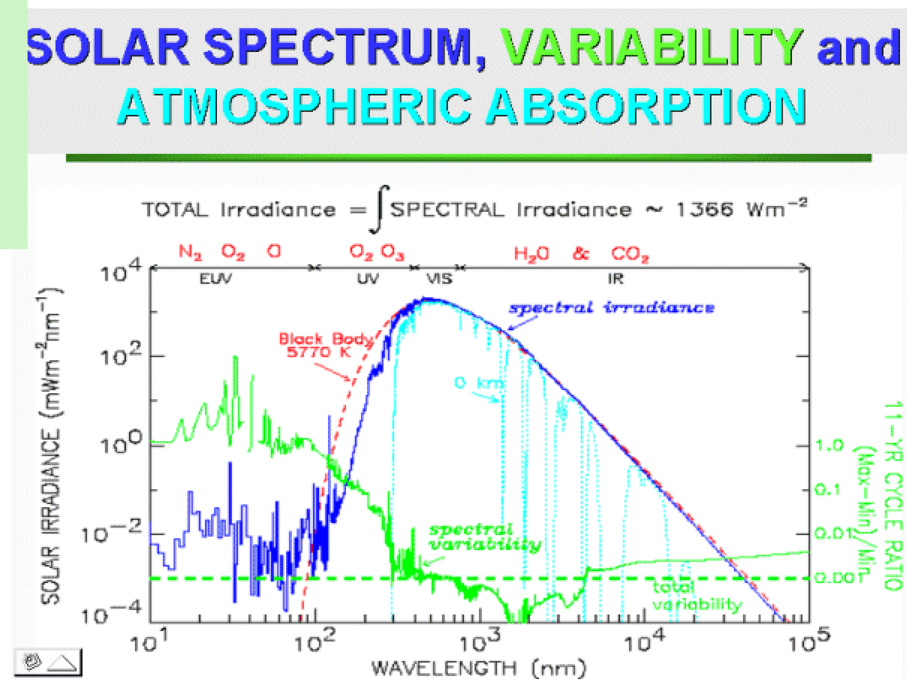

Broad band spectrum of the Sun (http://www.physics.unlv.edu/~jeffery/astro/sun/solar_spectrum_graph_2.html

2. Observational arguments in favor of two-phase accretion

I mentioned that the standard Keplerian disk does not always explain the broad band spectra of accretion objects. Now we will discuss several examples of this additional emission.

2.1 Active galactic nuclei

The broad band spectra of bright active galactic nuclei, without strong jets, can be schematically represented in the following way:

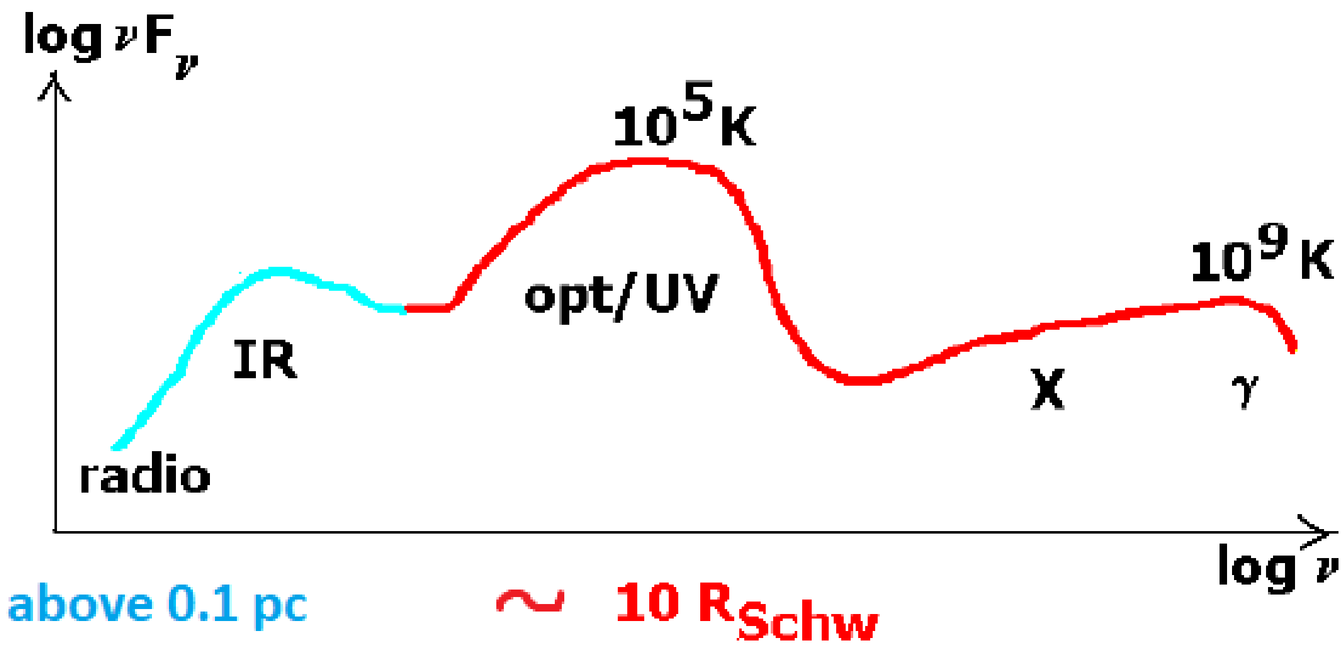

We know the rough distances from the black hole from time delays: UV/X-rays change roughly at the same time, further optical parts delayed by a few days, near-IR delayed 100 days, radio even more. Optical/UV part in bright sources is well represented by the Keplerian disk.

2.1 Active galactic nuclei

Schematically, a bright active galaxy looks in the folowing way.
The dusty/molecular torus forms a ring around the nucleus, at a distance of ~ 0.1 pc. It prevents to see clearly the nucleus from the side.
This torus is responsible for the near-IR emission, far-IR emission comes from still more distant regions, from the host galaxy.
The size of the dusty/molecular torus is measured through reverberation (time delays).

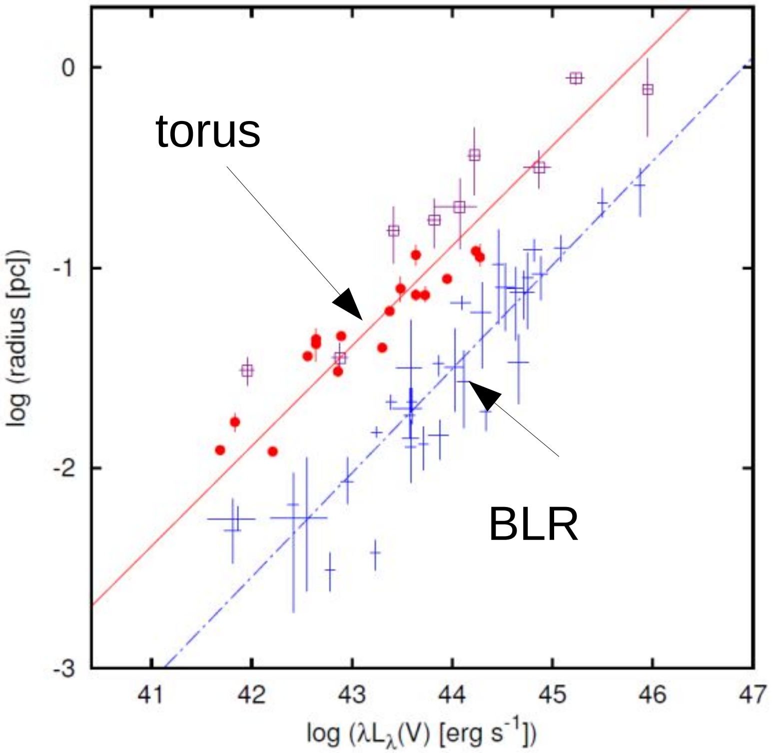

Measurements of the torus for nearby AGN from Koshida et al. (2014)

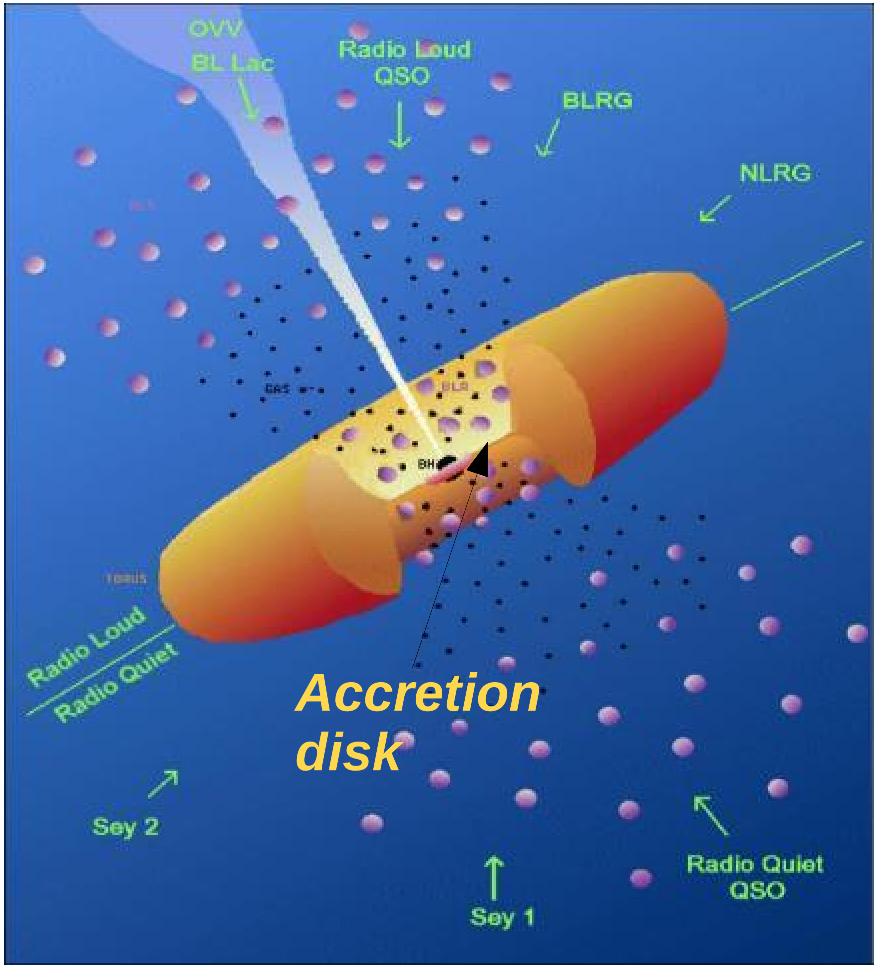

Schematic picture after Urry & Padovani (1995)

But where is the source of X-rays?

2.1 Active galactic nuclei

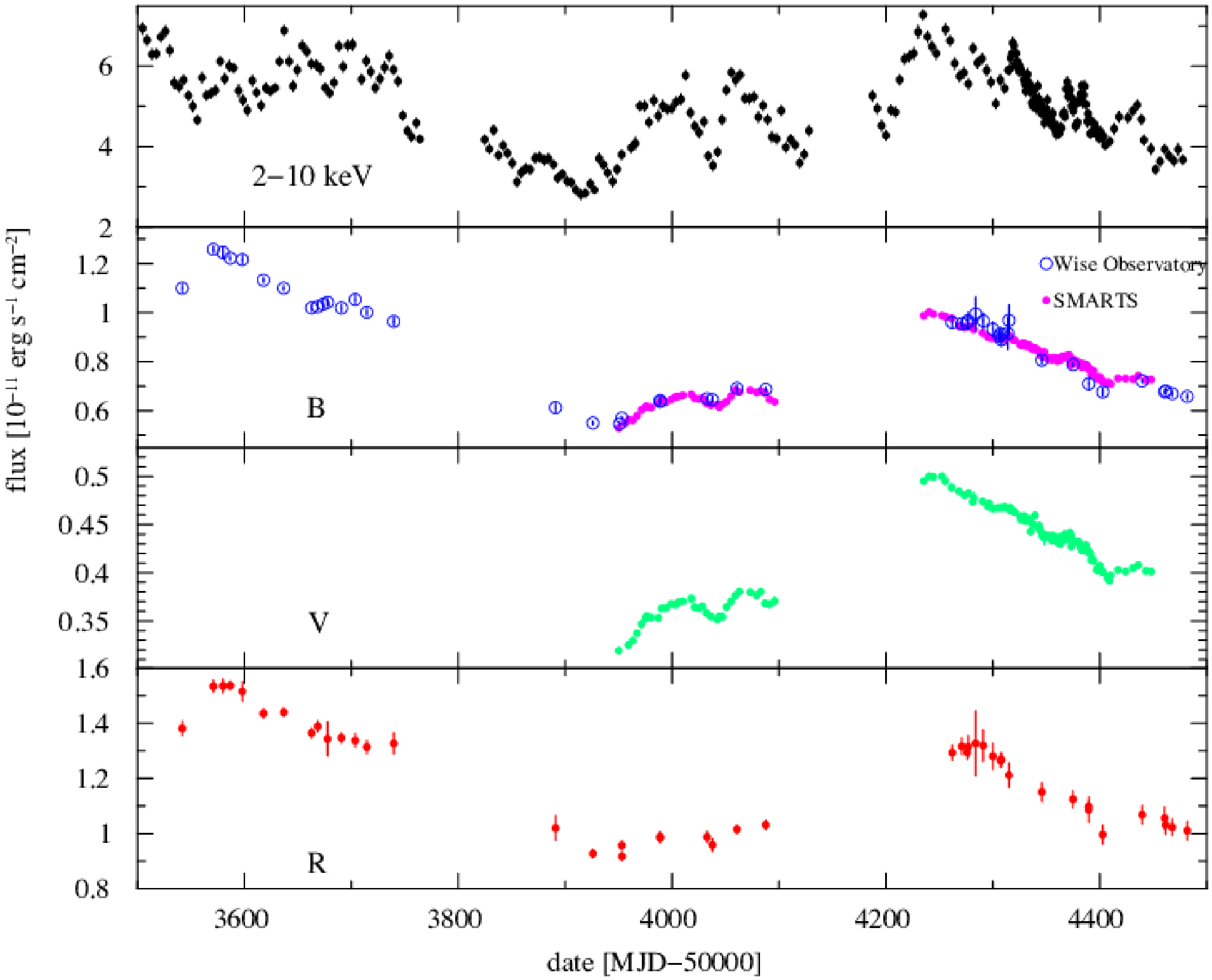

Radio-quiet AGN lightcurve (object: **MR 2251−178**, plot from Padovani 2017, after Arevalo et al. 2008) shows clearly that the X-ray emitting region is the most compact one since the variability is the fastest and the most violent.

Continuum emission does not allow for more precise description. We can have some insight paying attention to the line emission. We will briefly discuss this later.

2.2 X-ray binaries

In X-ray binaries sometimes the X-ray spectrum is disk-dominated, but sometimes it is not, and then it looks like a power law emission just like in AGN. We saw that during lecture 6.
But the cold medium is not restricted to the disk – additionally it can have a form of cold clouds. We see them in some highly inclined binary systems in absorption.

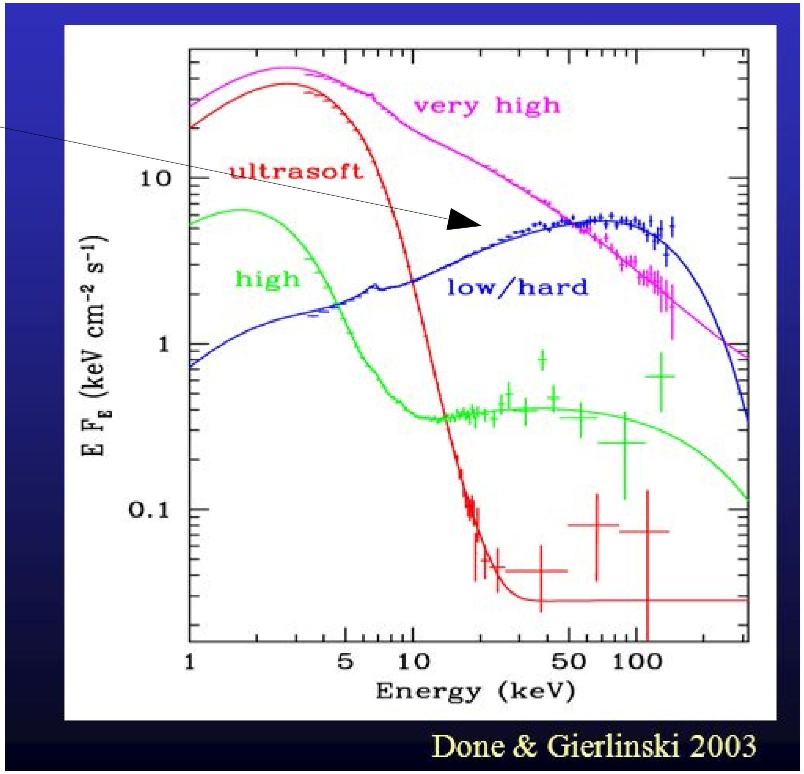

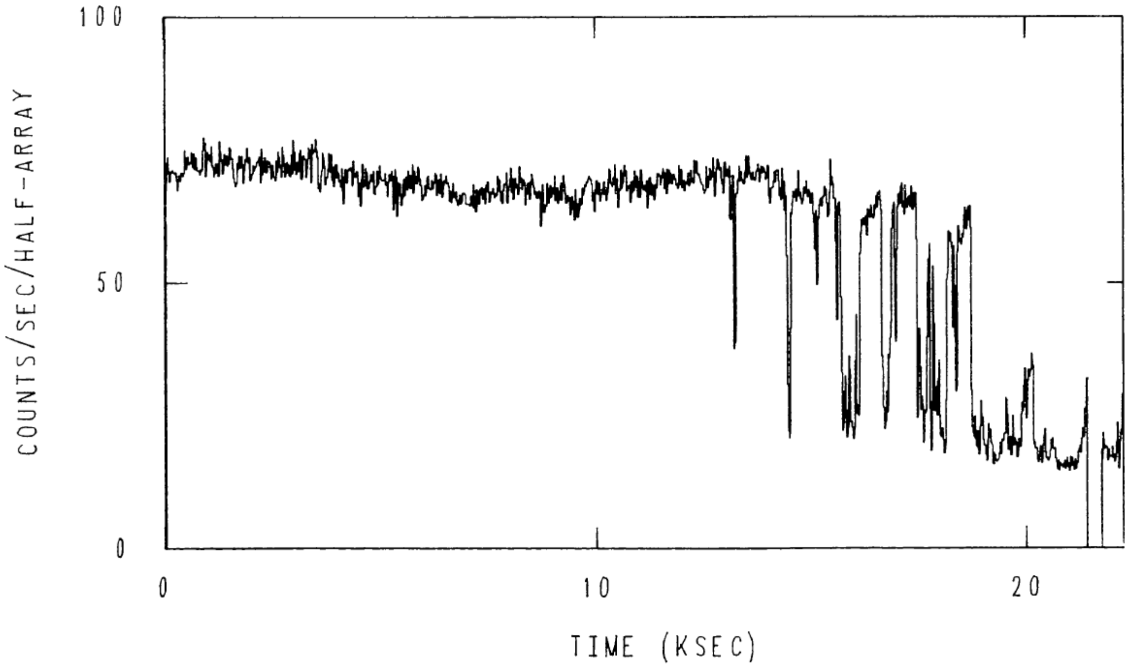

Figure 1. The complete EXOSAT ME X-ray light curve of 4U1624-49 (~2-10 keV) shown with 20s time resolution. Start time on this plot is 1984 March 5, 12:23 UT.

„Big Dipper" lightcurve from Watson et al. (1985).

Such lightcurves form due to the clumpiness of the outer edge of accretion disk, facing the companion and the stream comming from L1.

In AGN we also have colder clouds embeded in a hotter medium at larger distances – this is the Broad Line Region.

3. Mechanisms of production of the X-ray emission (continuum)

In order to understand the coexistence of the hot and cold plasma we have first to discuss the mechniasms of the production of X-ray continuum. The observed X-ray emission extends (in non-jetted sources) to 100 keV (corresponding to the temperature of 10^9 K). We showed during the lecture 2 that the expected maximum temperature of an accreting medium is 10^{12} K (virial temperature). Thus the key aspect if the cooling.

4.1 Otically thin thermal emission (free free, bremstrahlung)

In fully ionized thermal plasma ions and electrons are in equipartition, so the average thermal energy of the electron is the same as the average thermal energy of the ion. But ions are thousands times more massive (factor 1836 even for hydrogen). Thus protons move slowly, and are practically at rest in comparison to fast electrons ($E_k = 0.5\ mv^2$).

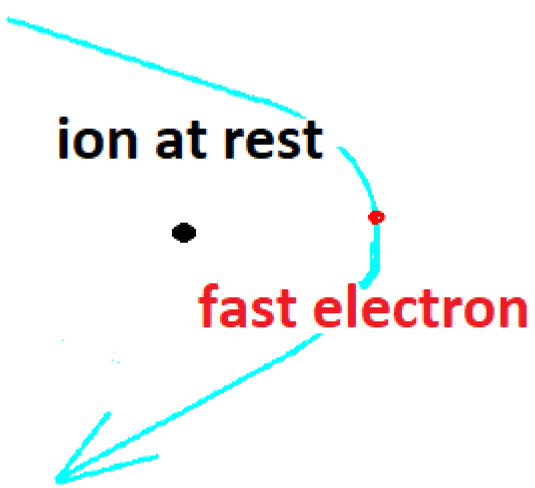

Coulomb interaction of the electron and the ion causes the electron to change the path, and acceleration leads to emission of an electromagnetic wave (photons). If the distribution of the electron velocities correspond to the temperature T, then the frequency-dependent emission is characterized by the formula

$$j_\nu^{ff} = 6.8 \times 10^{-38} Z^2 n_i n_e T^{-1/2} \exp\left(\frac{-h\nu}{kT}\right)$$

4.1 Optically thin thermal emission (free free, bremstrahlung)

The radiation flux is flat till we reach the photon energies comparable to the electron energies, when an exponential cut-off sets in.

$$j_\nu^{ff} = 6.8\times10^{-38} Z^2 n_i n_e T^{-1/2} \exp(\frac{-h\nu}{kT})$$

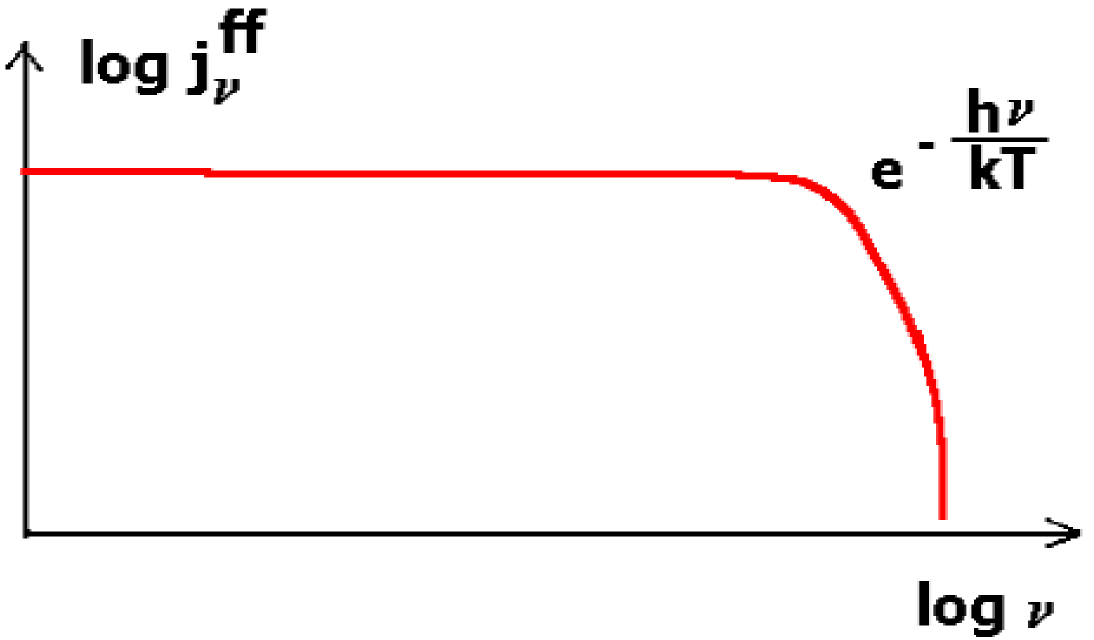

On νFν log-log diagram such a slope would correspond to slope +1. This is NOT what we see in AGN and X-ray binaries.

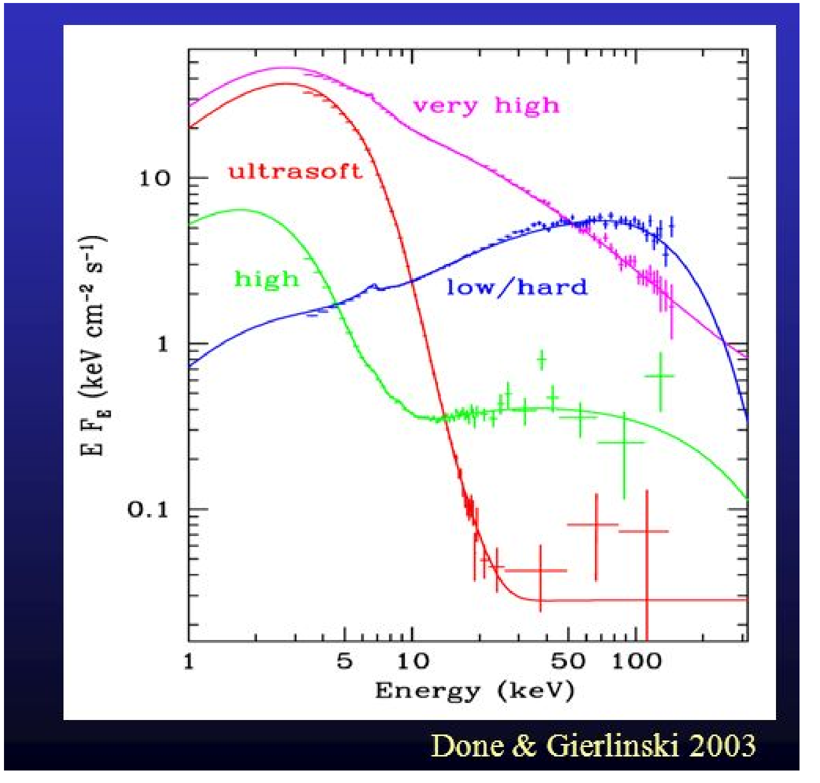

Done & Gierlinski 2003

But this mechanism is dominating in the solar corona, and in low accretion rate sources, and always it is a source of photons.
Emissivity integrated over frequency is

$$j^{ff} = 1.48\times10^{-27} Z^2 n_i n_e T^{1/2} g_B$$

where n gives the number density of ions and electrons, Z is the mass number of ions, and g_B is dimensionless factor. Emissivity scales with $T^{1/2}$.

4.2 Cyclotron and synchrotron emission

If we have a magnetic field, then electrons moving in this field, deflected by the Lorentz force will emit radiation. Characteristic cyclotron lines are visible in some atmospheres of **neutron stars**. If the electrons are relativistic, they emit synchrotron radiation. If electrons are thermal, then synchrotron emission is not very efficient. However, if electrons are non-thermal (accelerated in shock waves, with power-law dependence of the number of partcles at a given energy), then synchotron emission becomes very efficient. This emission mechanism is important for jetted sources.

Synchotron emission rarely extends to X-rays (it does for lower Eddington ratio sources, like BL Lacs)

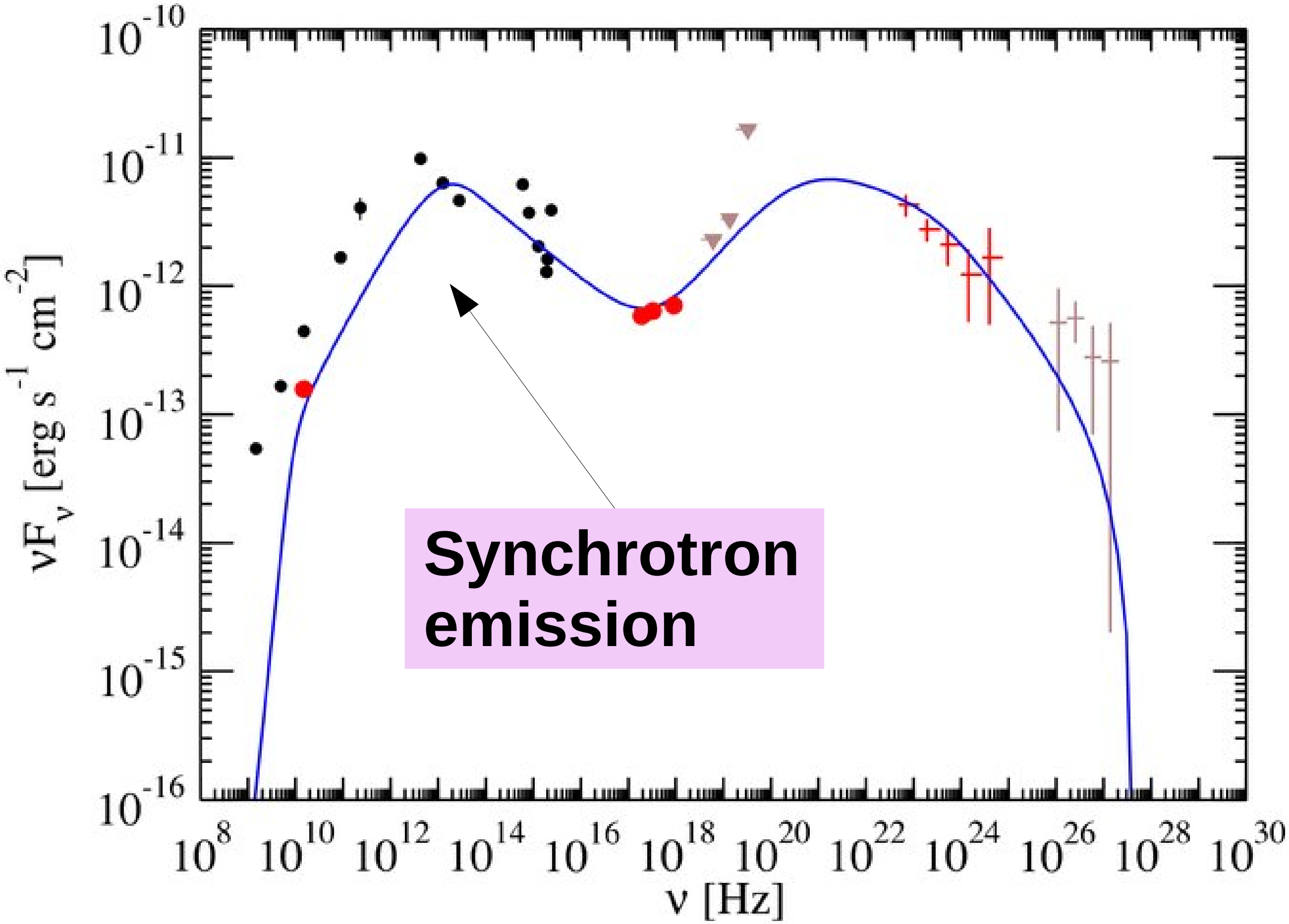

Broad band SED of M87 from Massaro (2009). The fitted spectrum represents the ***jet emission***

4.3 Compton process

(a) elastic (Thomson) scattering

We used it when determining the Eddington luminosity. Physically, the radiation is of similar nature to free-free emission but this time the oscillations of the electron are caused by the passing electromagnetic wave of a photon. Electron scattering is not isotropic.

The differential cross-section depends on the direction:

$$\frac{d\sigma_T}{d\Omega} \propto (1+\cos^2\theta)$$

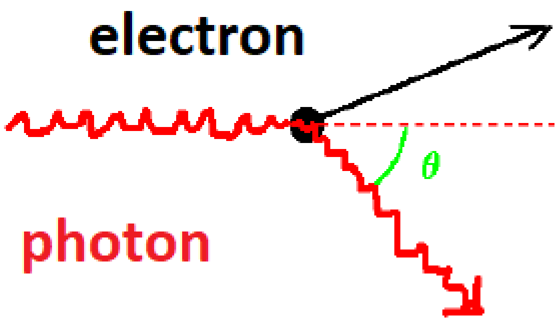

That is the scattered photon is more likely to go forward or backward than sideways, but the difference is not large (factor 2), so we usually use the cross-section integrated over the solid angle which we used before.

$$\sigma_T = \frac{8\pi}{3} r_o^2 \qquad r_o = \frac{e^2}{mc^2}$$

Here r_0 is the classical electron radius, we discussed that during the lecture 2. This cross-section does not depend on the photon energy, and electron here is assumed to be at rest.

In this approximation only the direction, and NOT the photon energy change.

4.3 Compton process

(b) inelastic (Compton) scattering

The previous approximation violates the conservation laws since in the scattering process we should conserve:

- Energy
- Momentum

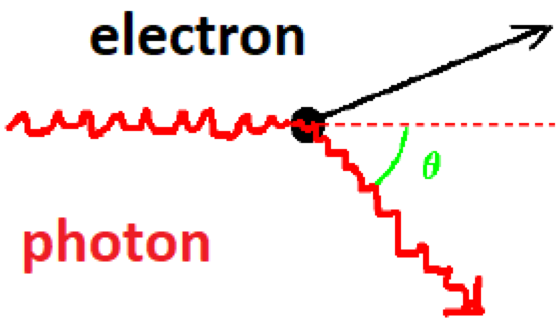

We need to write the energy balance before an after the interaction

$$E_\gamma + E_e = E'_\gamma + E'_e$$

Where the electron is initially at rest, so its energy is just $m_e c^2$, and after the scattering its energy contains also the momentum part (we allow for the relativistic motion of the electron after scattering)

$$E'_e = \sqrt{(m_e c^2)^2 + (p'_e c)^2}$$

This is why in the final form the electron mass appears. Conservation of momentum requires vector approach (separately the component paraller and vertical to the initial directoion of the photon motion), and the scattering angle θ appears. The formula for the photon energy after the scattering is:

$$E'_\gamma = \frac{E_\gamma}{1 + \frac{E_\gamma (1 - \cos\theta)}{m_e c^2}}$$

4.3 Compton process

This formula simplifies if we use the wavelength instead of energy

$$E_\gamma = h\nu = h\frac{c}{\lambda}$$

$$E'_\gamma = \frac{E_\gamma}{1 + \frac{E_\gamma(1-\cos\theta)}{m_e c^2}}$$

We then obtain the relation:

$$\lambda' - \lambda = \frac{hc}{m_e c}(1-\cos\theta)$$

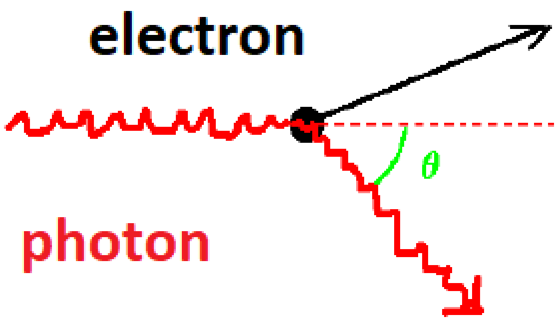

In the most famous form. But the energy form has its advantages since it allows to see more directly the fractional change of the energy.

For example, if we assume that
- The angle is 90 deg (i.e. cos θ = 0)
- The change of the energy is small

Then we obtain a rough estimate for the photon energy loss in a single scattering

$$\frac{\Delta E_\gamma}{E_\gamma} = -\frac{E_\gamma}{m_e c^2}$$

Which shows that the energy change of the photon is indeed small if its initial energy is much smaller than the rest energy of the electron.

At E_γ close to $m_e c^2$ we have to include exact formula, and in addition quantum effects decrease the cross-section (Klein-Nishina effect). It actually slowly sets-in at 50 keV ($m_e c^2$ = 511 keV).

Now we will consider an option of the energy gain by the photon.

4.3 Compton process

In previous derivation we assumed that the electron is at rest before the scattering with photon. But in a hot plasma electrons can have large energies, actually much larger than the photon energy.
The general formula is derived simply by first going to the rest frame of the electron performing Lorent transformations appropriate for the Special Relativity

$$E_\gamma' = \gamma E_\gamma (1 - \beta \cos\theta)$$

Which basically boost the electron energy by a factor γ, and we do it twice (we have to return to the original observer's frame, thus the amplification goes as $1:\gamma:\gamma^2$, and the photon gains energy in each scattering.
If we assume that the velocity of electrons corresponds to a thermal plasma (Maxwell distribution) then the photon energy gain in each scattering is determined by the plasma temperature

$$\frac{\Delta E_\gamma}{E_\gamma} = \frac{4kT}{m_e c^2}$$

This is a non-relativistic formula, correct when $kT << m_e c^2$

This phenomenon is frequently called **Inverse-Compton process**. In reality, Compton process sometimes cool and sometimes heats plasma, and we can conveniently combine this formula with the previous one to have a general prescription for the energy gain by photon in a single scattering:

$$\frac{\Delta E_\gamma}{E_\gamma} = \frac{4kT - E_\gamma}{m_e c^2}$$

5. Comptonization and the spectrum formation

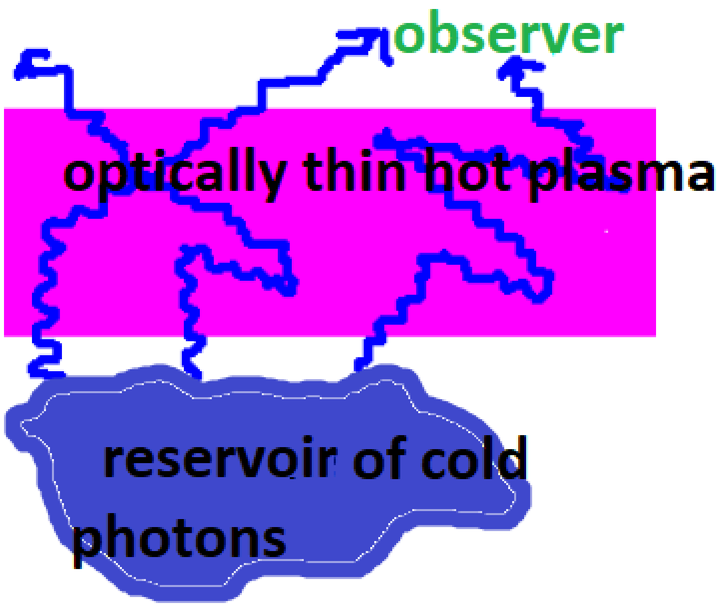

If we have a reservoir of cold photons (for example, from the Keplerian disk), and nearby there is a very hot plasma, photons will gain energy in each subsequent scattering according to $\frac{\Delta E_\gamma}{E_\gamma} = \frac{4kT}{m_e c^2}$

But finally their temperature will approach 4 kT,

$$\frac{\Delta E_\gamma}{E_\gamma} = \frac{4kT - E_\gamma}{m_e c^2}$$

and there the energy gain will stop. The final spectrum will qualitatively look like this

The formulae on the left are approximate, and the actual saturation depends on the optical depth of the medium: for optically thin medium the turn-off is at kT, for optically thick medium at about 3 kT.

The slope of the power low depends on the energy gain in each scattering, and on the probability of the subsequent scattering.

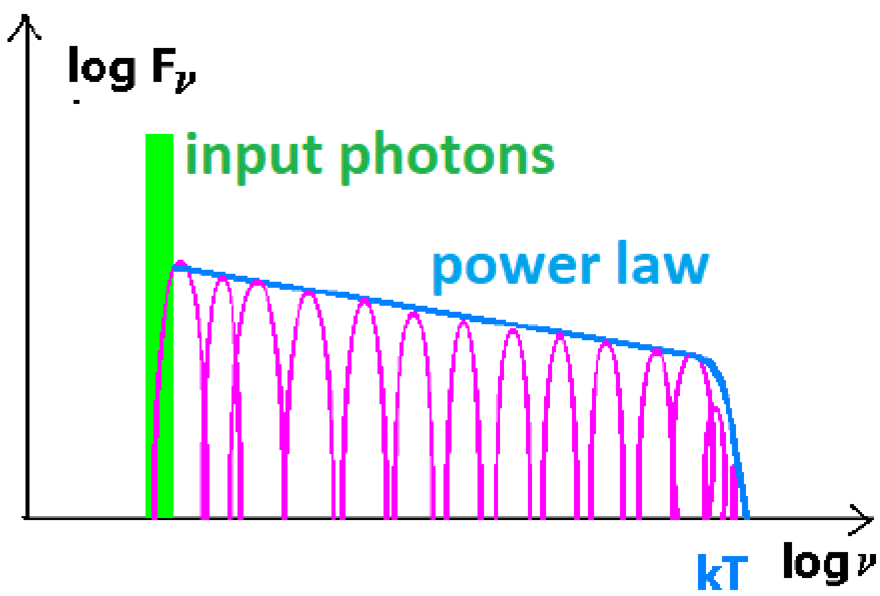

5. Comptonization and the spectrum formation

We can describe the net cooling effect quantitatively. Assuming that the medium is optically thin we can write the electron cooling rate (photons gain the energy) per unit volume

$$Q = F \sigma_T n_e \frac{4kT - E_\gamma^{mean}}{m_e c^2}$$

It we are interested in Comptonization by a slab of a fixed optical depth $\tau = \sigma_T n_e H$ where H is the geometrical depth of the medium, then the relative gain of the energy by the photon is given by the gain in a single scattering and the number of scatterings.

As we saw in lecture 2, the number of scatterings in general case (both optically thick and optically thin medium) is described by the bridge formula τ(τ+1). So the important parameter in the consideration of the expected X-ray spectral slope is the Compton parameter

$$y = \frac{\Delta E_\gamma}{E_\gamma} \tau(\tau + 1)$$

Here we can use the formula from the previous page to determine a single gain.

If the Compton parameter of the medium is smaller than 1 the Comptonization is called unsaturated, and the power law spectrum forms. Most of the photons do not reach the maximum energy.

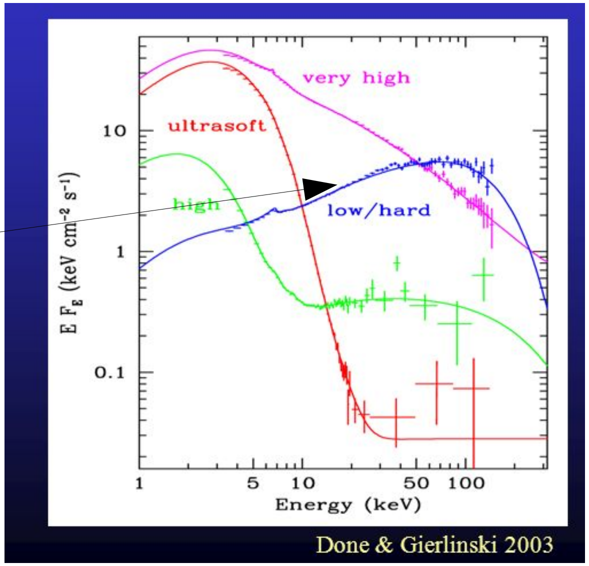

5. Comptonization and the spectrum formation

We can describe the net cooling effect quantitatively. Assuming that the medium is optically thin we can write the electron cooling rate (photons gain the energy) per unit volume

$$Q = F \sigma_T n_e \frac{4kT - E_\gamma^{mean}}{m_e c^2}$$

It we are interested in Comptonization by a slab of a fixed optical depth $\tau = \sigma_T n_e H$ where H is the geometrical depth of the medium, then the relative gain of the energy by the photon is given by the gain in a single scattering and the number of scatterings.

As we saw in lecture 2, the number of scatterings in general case (both optically thick and optically thin medium) is described by the bridge formula $\tau(\tau+1)$. So the important parameter in the consideration of the expected X-ray spectral slope is the Compton parameter

$$y = \frac{\Delta E_\gamma}{E_\gamma} \tau(\tau + 1)$$

Here we can use the formula from the previous page to determine a single gain.

If the Compton parameter of the medium is greater than 1 and the medium itself provides photons in the form of a free-free emission then much more complex spectrum forms.

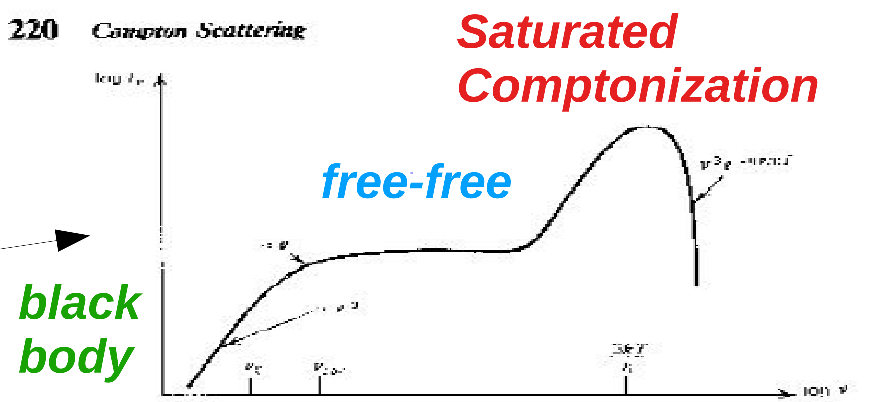

Figure 7.4 Spectrum from a thermal, nonrelativistic medium characterized by free-free emission and absorption and by saturated inverse Compton scattering. At low frequencies the spectrum is blackbody then becomes modified blackbody and, at high frequencies, becomes a Wien spectrum.

From Rybicki & Lightman

6. Matter in equilibrium with radiation – Inverse Compton temperature

If we strongly irradiate optically thin medium which is unable to cool through atomic processes it will reach and equilibrium between Compton heating and Compton cooling

$$\frac{\Delta E_\gamma}{E_\gamma} = \frac{4kT - E_\gamma^{mean}}{m_e c^2}$$

$$4kT_{IC} = E_\gamma^{mean}$$

$$E_{mean} = \frac{\int_0^\infty F_\nu h\nu \, d\nu}{\int_0^\infty F_\nu \, d\nu}$$

Note that Inverse Compton temperature does not depend on the radiation flux, just on the radiation spectrum.

For a typical broad band spectrum of AGN or GBH the Inverse Compton temperature is of order of 10^7 – 10^8 K.

Such a medium may form when the outer parts of the accretion disks are exposed to strong irradiation by the central parts. The temperature does not depend on the flux, and thus is independent from the distance.

Thus irradiation may lead to formation of an outer corona (when $kT_{IC} < T_{vir}$), and finally to the wind (when $kT_{IC} > T_{vir}$). Such corona/winds are present in galactic sources (Accretion Disk Corona sources – ADC).

Such corona does not produce much emission but it is important for eclipsing sources, since it scatters the central flux.

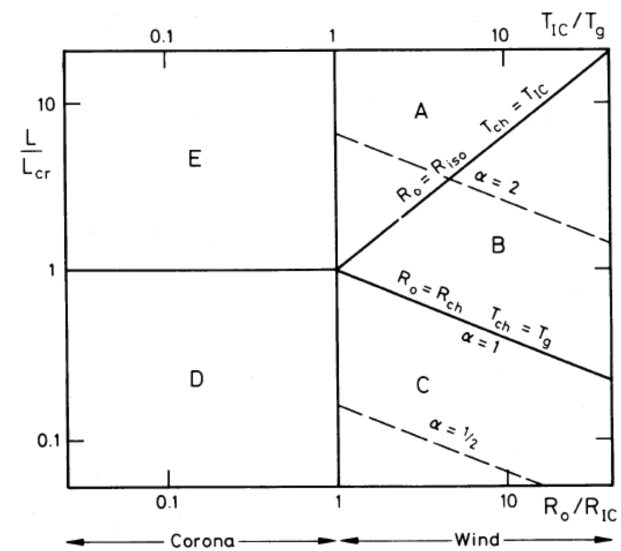

FIG. 1.—Parameter space for Compton-heated winds from accretion disks. The radius R_0 at which a streamline originates on the

Begelman et al. (1983)

7. The location of the X-ray emitting hot medium

We know (from variability) that most of the X-ray emission in radio-quiet sources must come from the compact region close to a black hole, and we know (from broad band spectra) that the fraction of energy dissipated in this form is noticeable (from about 10% in some quasars up to 30% in other quasars, and more in low Eddington ratio sources). We know that the cooling is through Comptonization (from the power law shape). But we do not know

- The heating mechanism
- The geometry

Haeting must be related somehow to accretion but we cannot easily trance the geometry. The shape of the Comptonized spectrum is not sensitive to geometry. So there are various ideas.

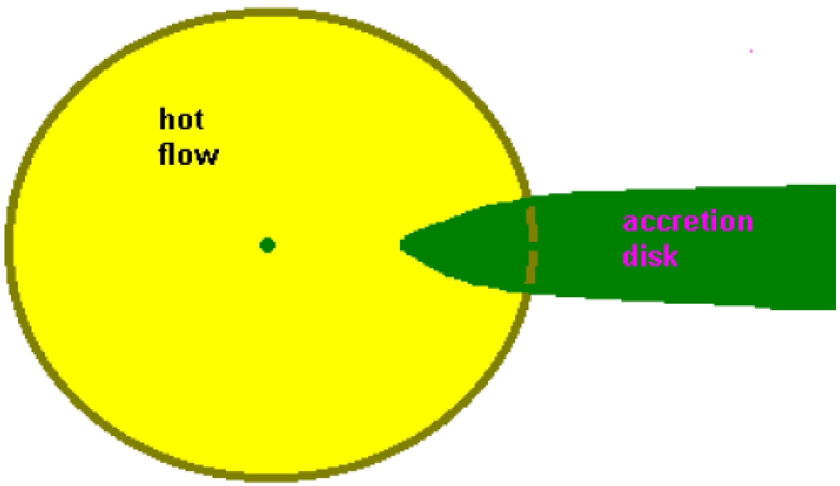

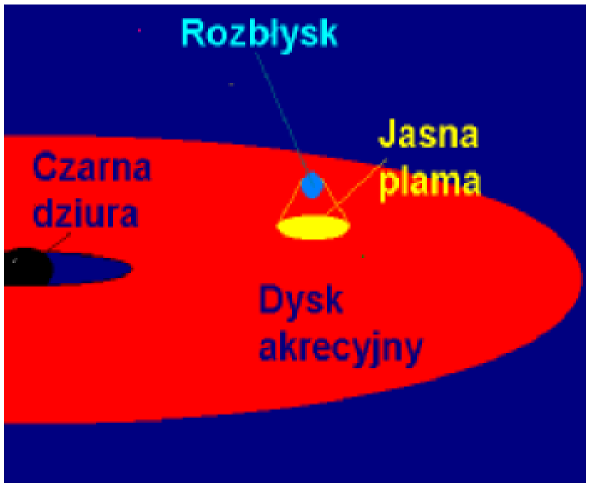

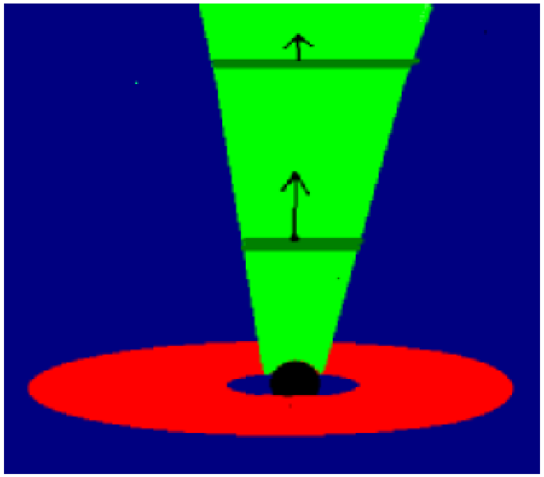

Inner hot flow

Magnetic flares

Jet emission

7. The location of the X-ray emitting hot medium

Each of these geometries has some justification, so quite likely the real geometry is a combination of all these:

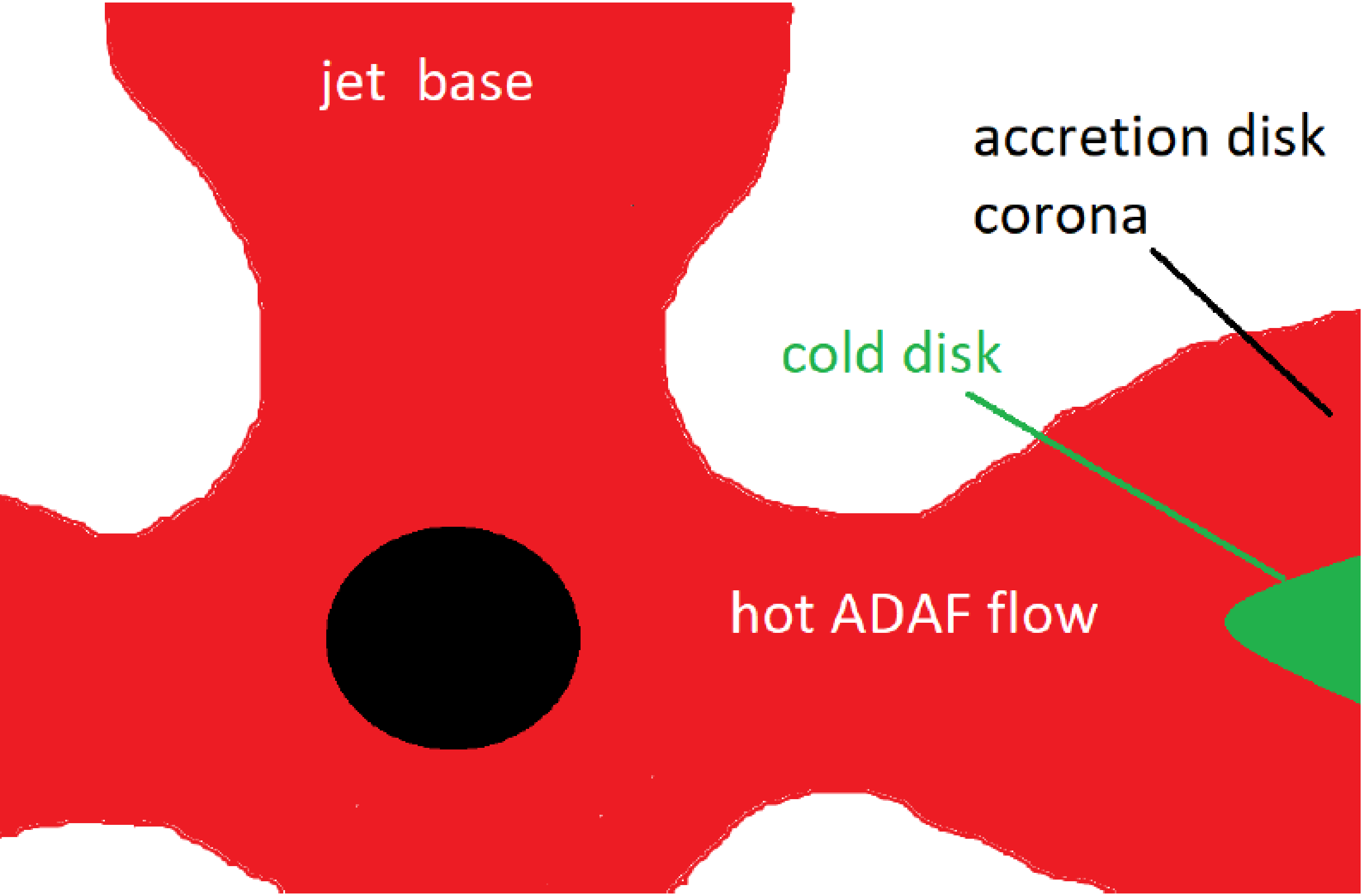

The relative importance of elements strongly depends on the Eddington ratio (in general, for lower Eddington ratios the cold disk recedes or disappears), but the issue is still a mettre of debate because we do not have the complete theory of the transition from the cold optically think flow to the hot optically thin plasma, and we do not know the plasma dynamics.

8. Tracing geometry with the use of the atomic physics and the hot plasma/cold disk interaction

Cold accretion disk is actually partially ionized, and thus it is a source of atomic features, for example emission lines. Emission lines allow to determine observationally the projected velocities using the Doppler effect. In the disk we actually know the velocity field. The formation of lines is strongly coupled to the way how the hot plasma interacts radiatively with the colder material.

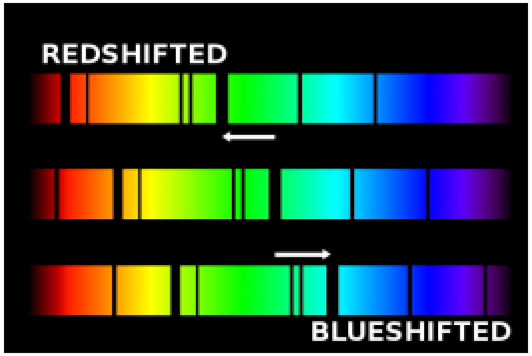

Samihah's Astronomy Blog

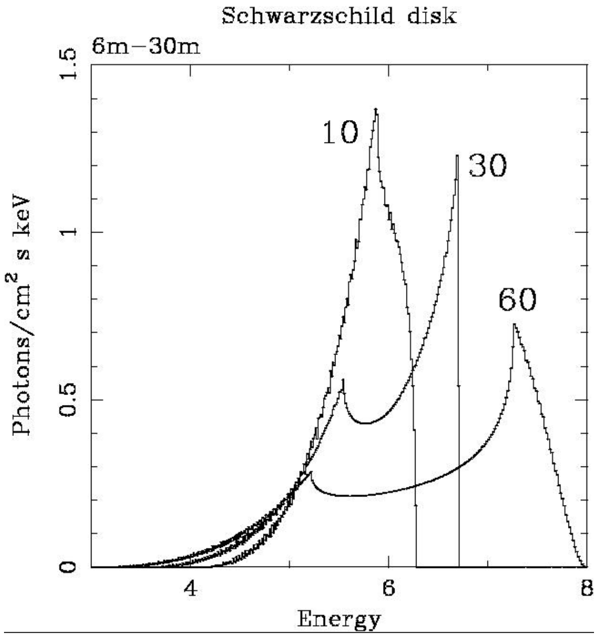

Lines from accretion disks extending from ISCO to 15 Rschw From Fabian et al. (2000)

We have to look at the radiative interaction since physical contact is more difficult to analyse:

- Hot matter if in contact with cold matter should be roughly in pressure equilibrium but this is easily satisfied through the corresponding density contrast $\rho_1 T_1 = \rho_2 T_2$
- The role of thermal conduction is not quite clear also was used in some attemts to get the hot/cold plasma transitions (e.g. Różańska & Czerny 2000)

8. Tracing geometry: Active galactic nuclei

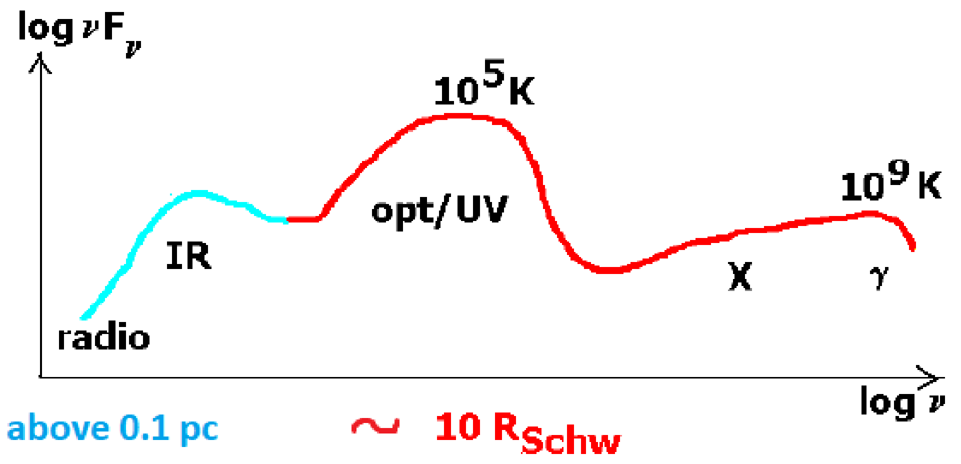

If we seek more precisely into the X-ray band we will see something like that

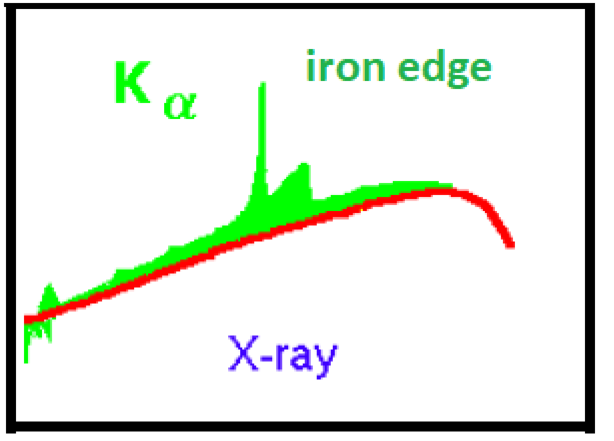

This green feature is an iron line, and an iron edge produced as a result of the reprocessing of the X-ray continuum at the surface of the cold accretion disk.

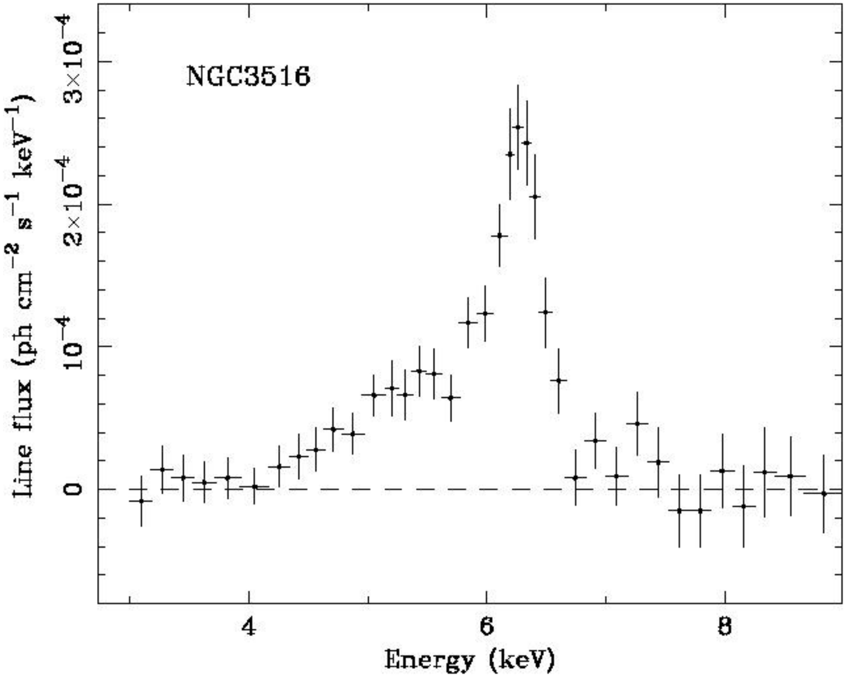

An example of the emission excess above a local power law (Fabian et al. 2000) https://ned.ipac.caltech.edu/level5/Fabian4/Fab2_3.html)

8. Tracing geometry: Active galactic nuclei

The mechanism of the iron line production is the following:

- X-ray continuum radiation falls onto a cold disk which contains neutral (or weakly ionized) iron atoms.
- One of the photons may be aborbed and it will remove an electron from the inner shell K of iron atom; this electron escapes
- An empty hole is now at shell K
- An electron from the shell L jumps to shell K, which leads to an emission of the photon with energy corresponding to the energy difference between the two shells, this energy is 6.4 keV
- The probability of this process is actually only 24 %, in the remaining cases the ionized atom rearranges it shells without emission of a photon, but instead with an emission of an electron (Augere process)

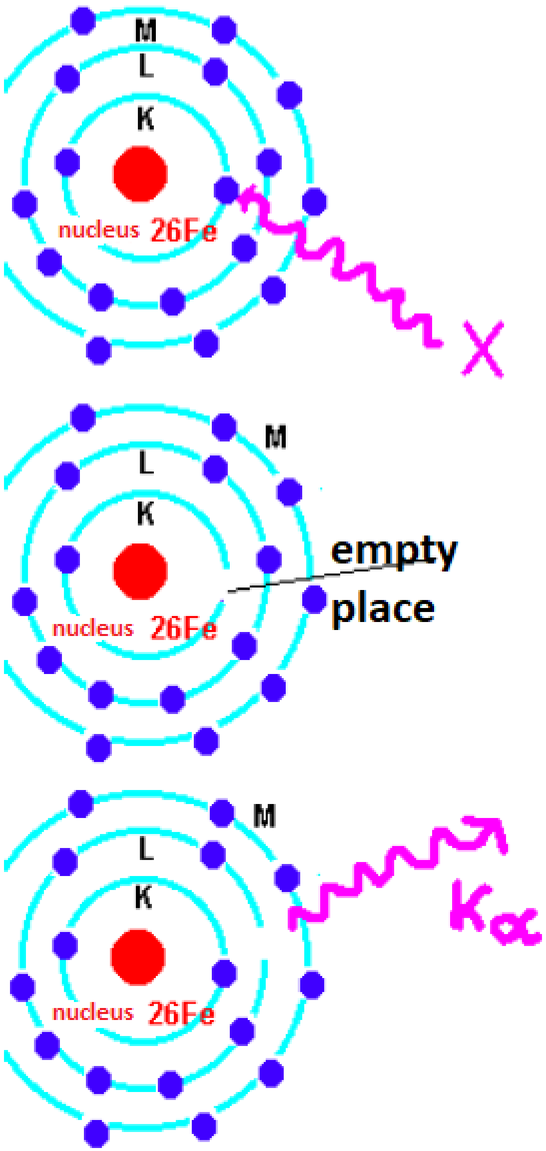

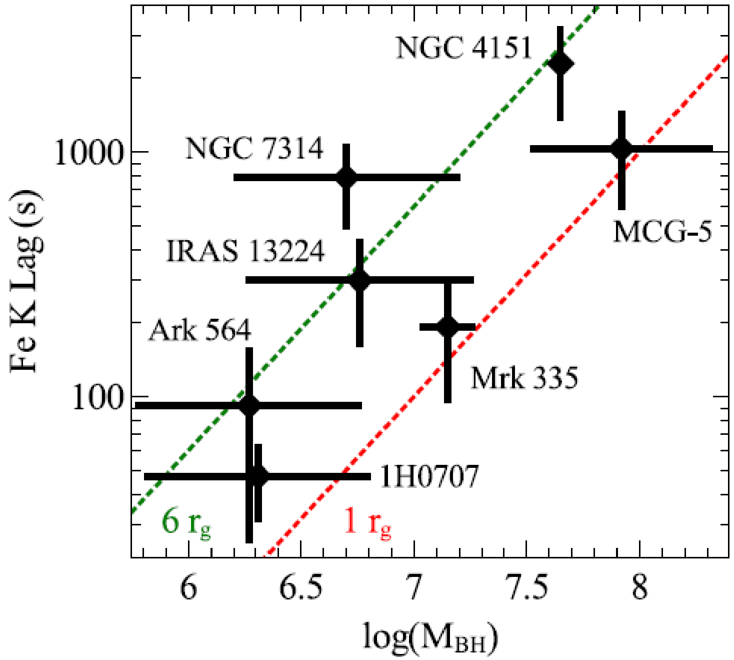

The delay between the disk emitting Kα line with respect to continuum is very short, 100-1000 seconds only!

Delays from Kara et al. (2013)

8. Tracing geometry: Active galactic nuclei

The shape of the line is consistent with **the motion of the Keplerian disk** in its innermost parts (at least in some sources), and allows to measure the black hole spin.

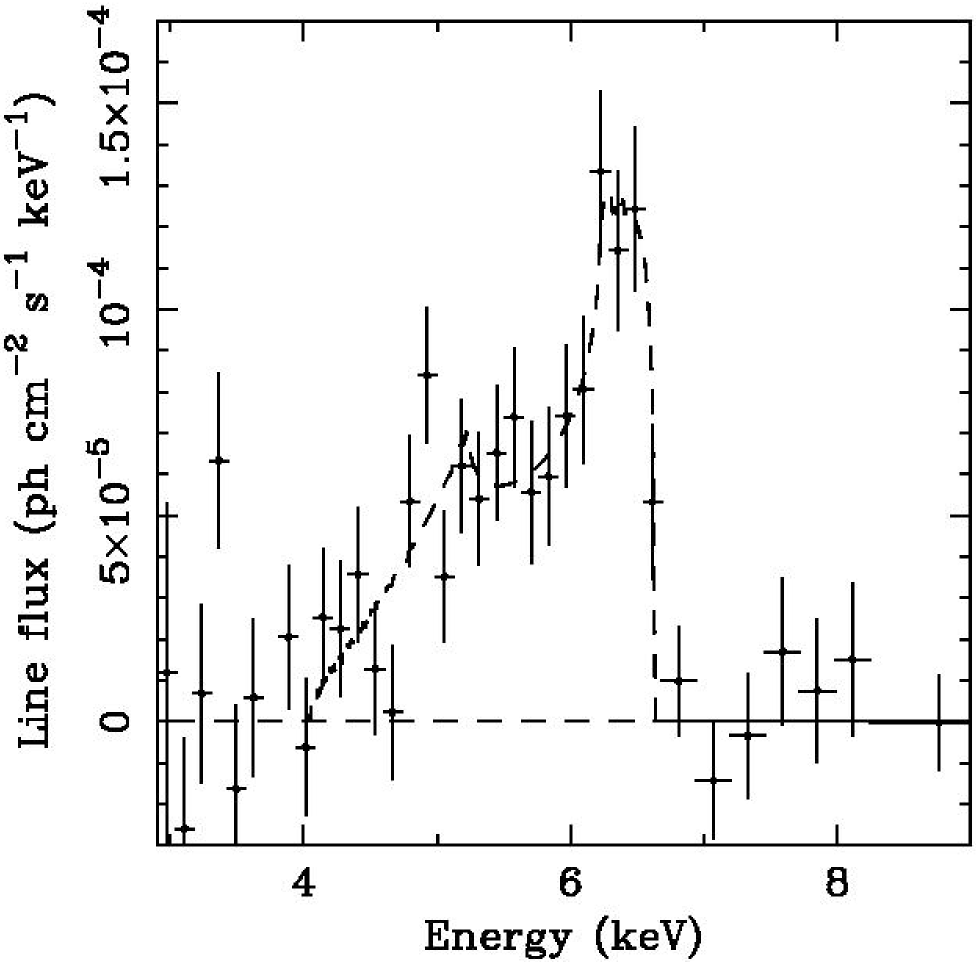

ASCA detection of the broad Kα line (Iwasawa 1995)

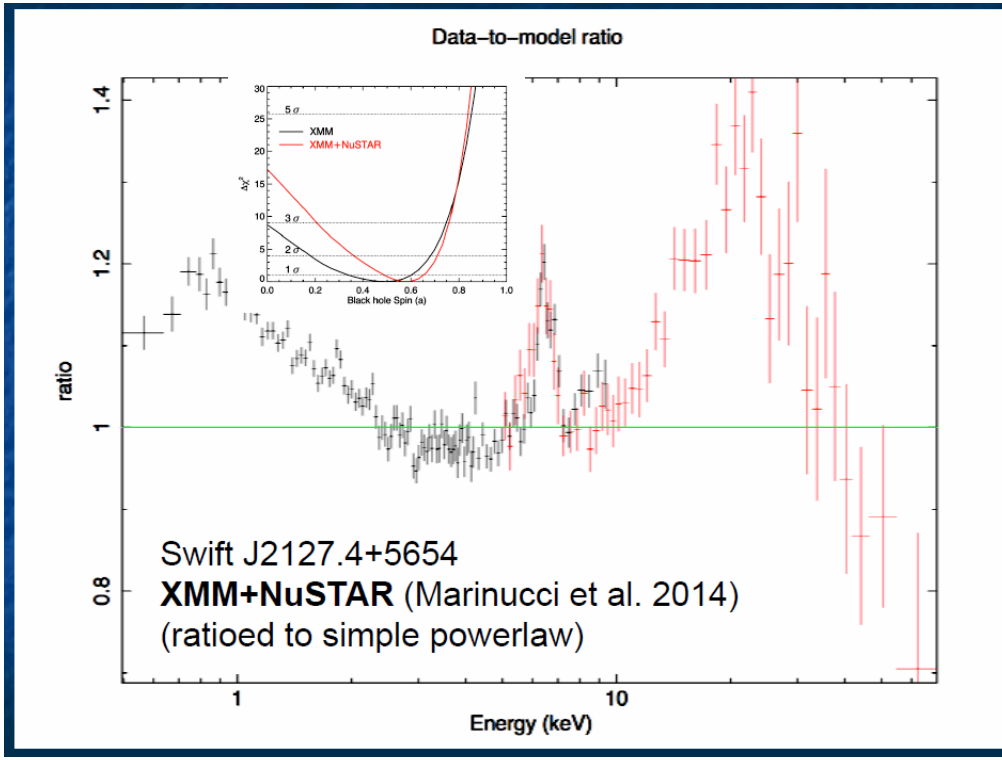

The X-ray continuum emitting region has to be also quite compact (in these sources).

8. Tracing geometry: X-ray binaries

In X-ray binaries sometimes the X-ray spectrum is disk-dominated, but sometimes it is not, and then it looks like a power law emission just like in AGN. We saw that during lecture 6. When the spectrum is of the power law character, it shows exactly the same iron line, which forms again very close to the black hole.

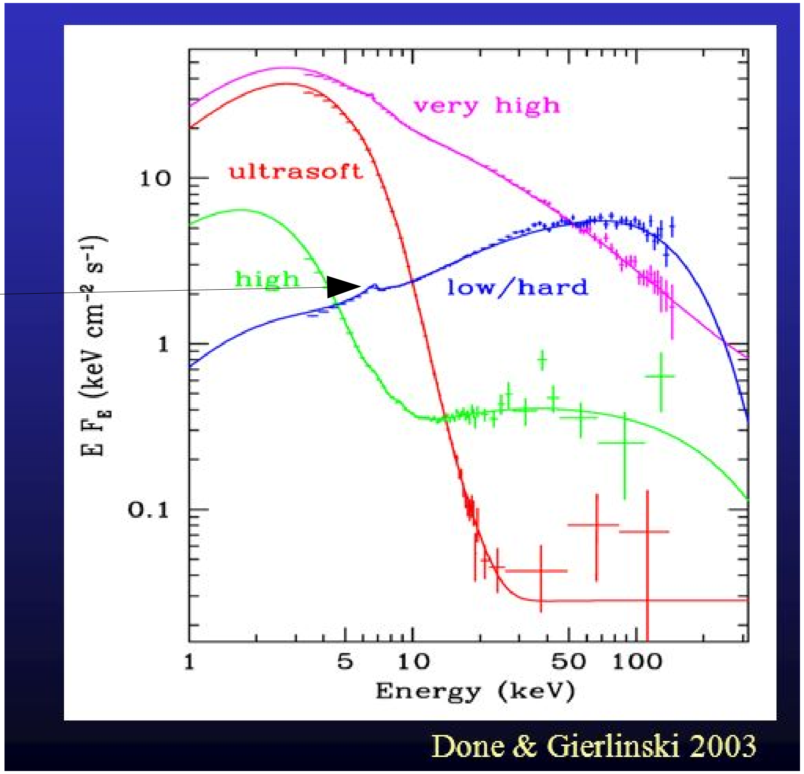

Also sources with neutron stars show similar, relativistically broadened iron line.

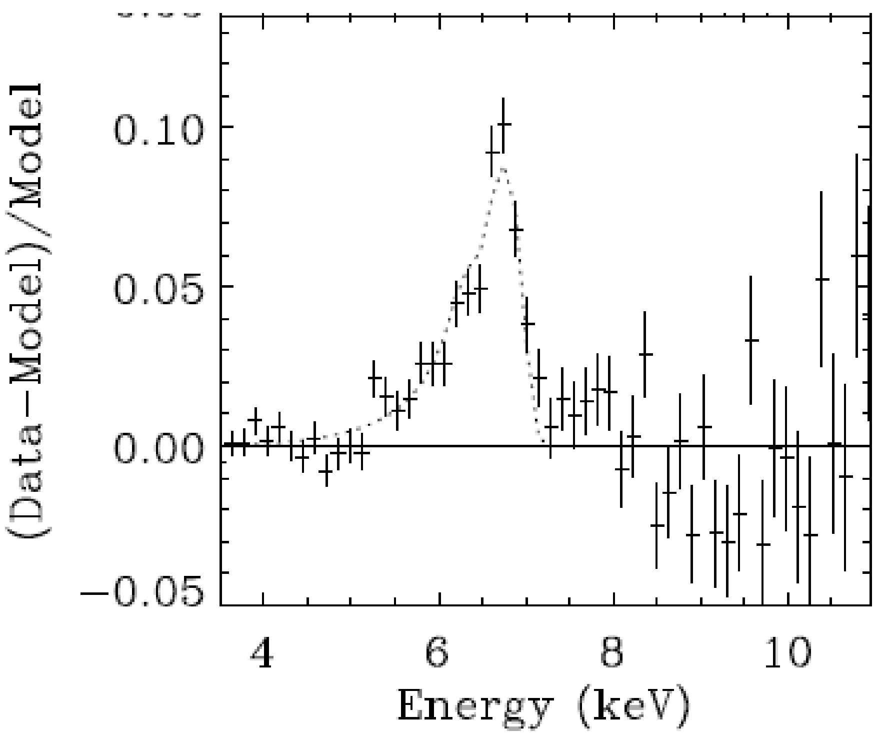

Ser X-1 from Bhattacharyya & Strohmaier (2007), a source containing a neutron star.

There is still an on-going discussion if the disk extends down to ISCO in a luminous hard state, or not, since different authors get different results which also implies different concusion about the hot phase geometry.

8. Tracing geometry: X-ray binaries

For example, studying the reprocessing of the compact corona by the disk during the outburst of the black hole transient Kara et al. (2019) argues that the corona shrinks after the strong outbursts (data from NICER).

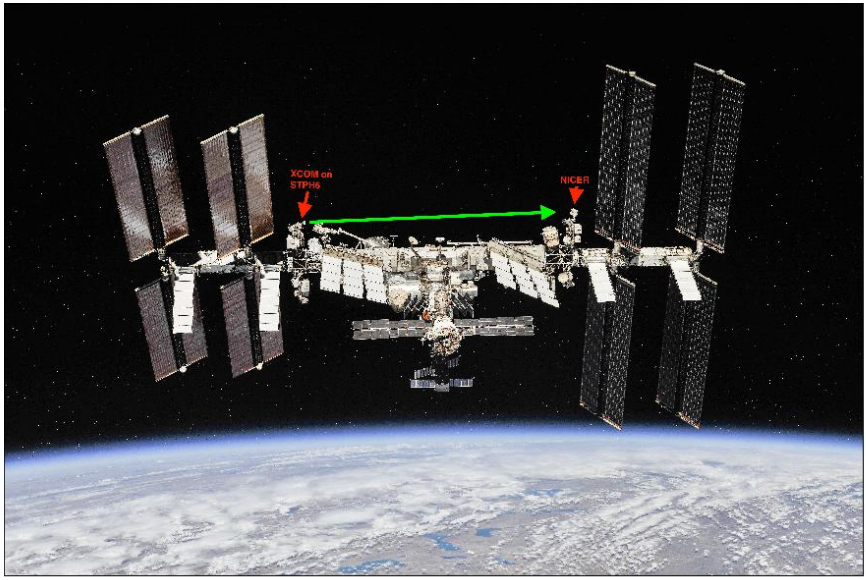

NICER- instrument on board of the ISS (International Space Station)

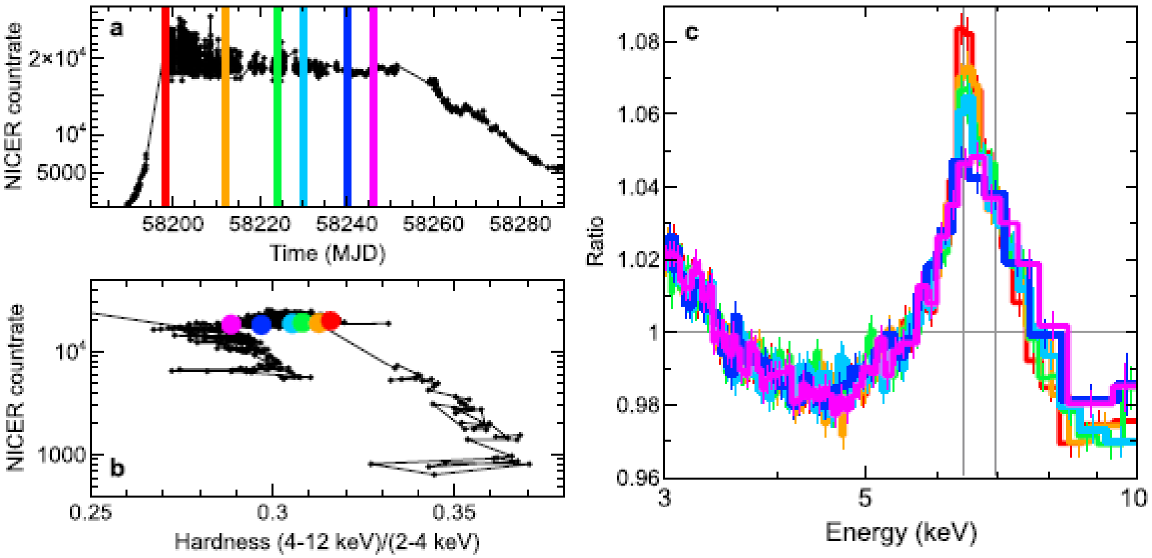

Figure 1. Overview of MAXI J1820+070 in the hard state. (a) The long term 0.2-12 keV NICER

Conclusion about the geometry

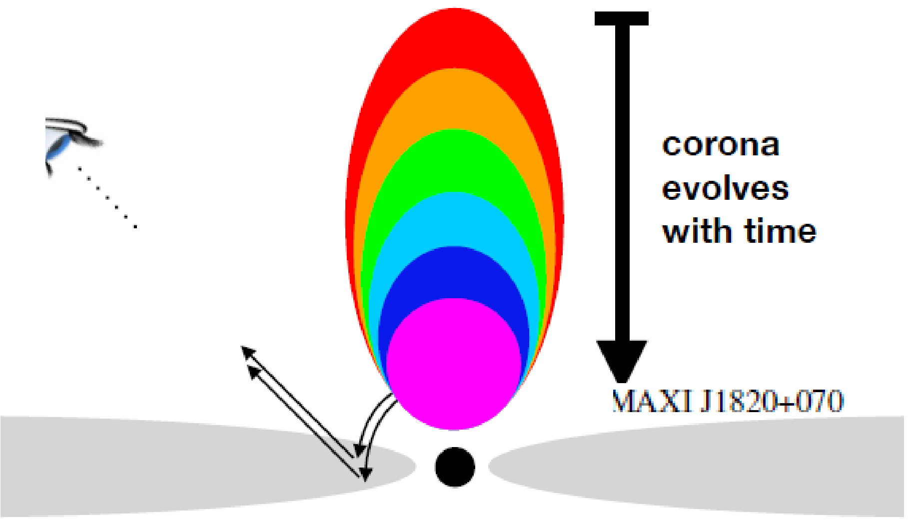

Figure 4. Schematic of the proposed geometry. Schematic of the proposed geometry, evolving from a vertically extended corona at early times, to a more compact corona at late times. The constant shape of the broad iron line is due to a static core of the corona at small radii that is responsible for most of the flux

8. Tracing geometry: X-ray binaries

However, the methods based on reprocessing do not provide unique answers, if you compare the results for the same source obtained by different people from the same data. Here is an example:

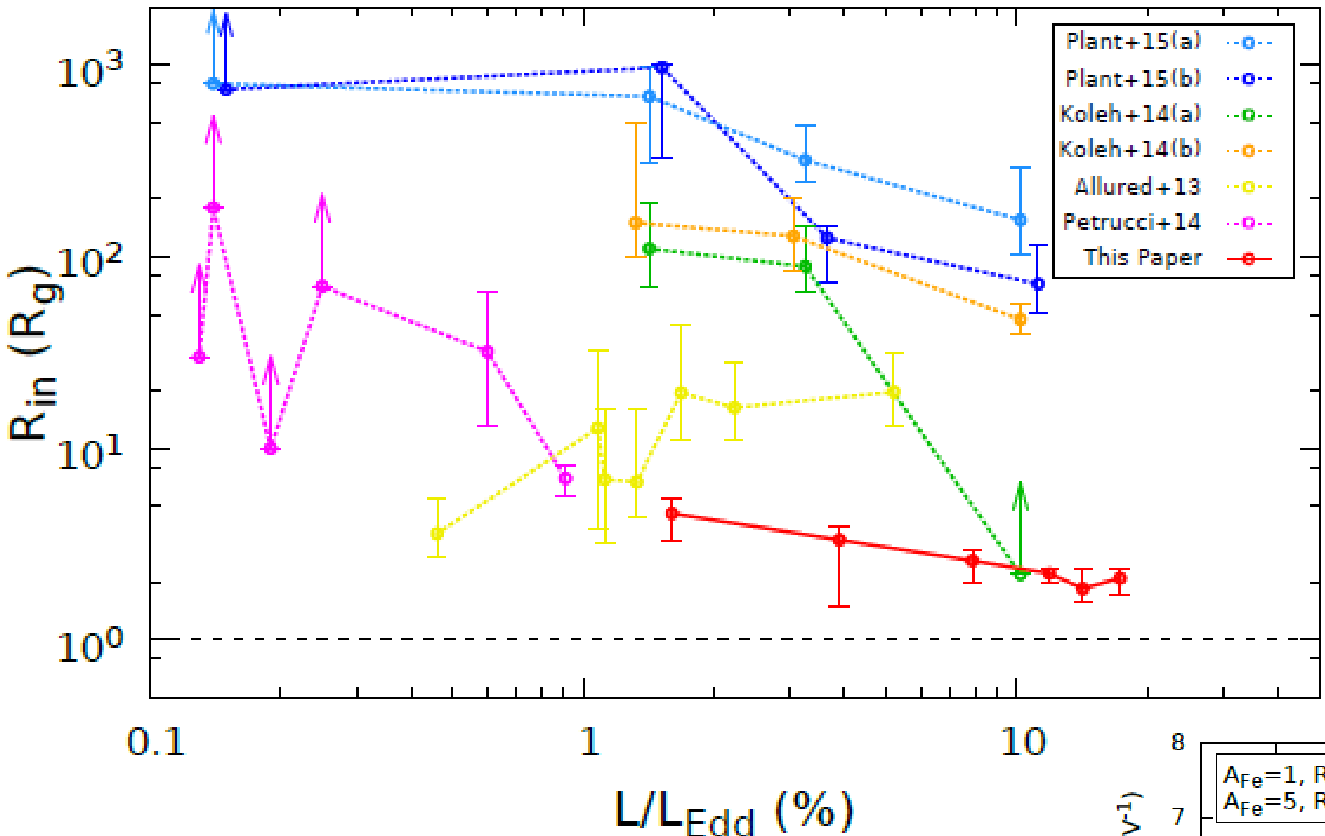

The position of the inner edge of the Keplerian disk during the outbursts of BHB GX 339–4 (Garcia et al. 2015)

The authors stress the degeneracy of the solutions with respect to some parameters which may explain the problem.

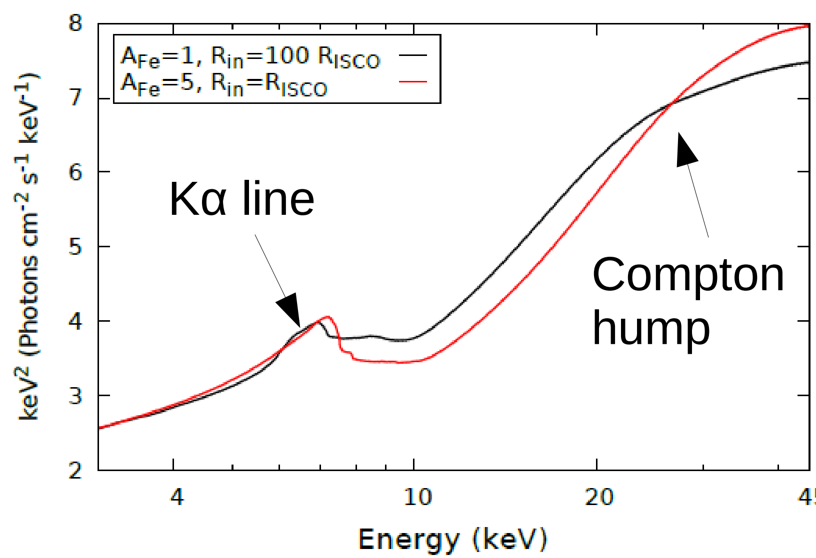

9. Compton hump

Irradiation of the cold disk by X-ray continuum leads to formation of the iron line (and other iron lines, other highly ionized lines, comming from CNO elements). But part of the photons are not absorbed, but scattered almost like in thermal Comptonization.

Relativistic reflection

From presentation by Svoboda (2014) done for Athena mission

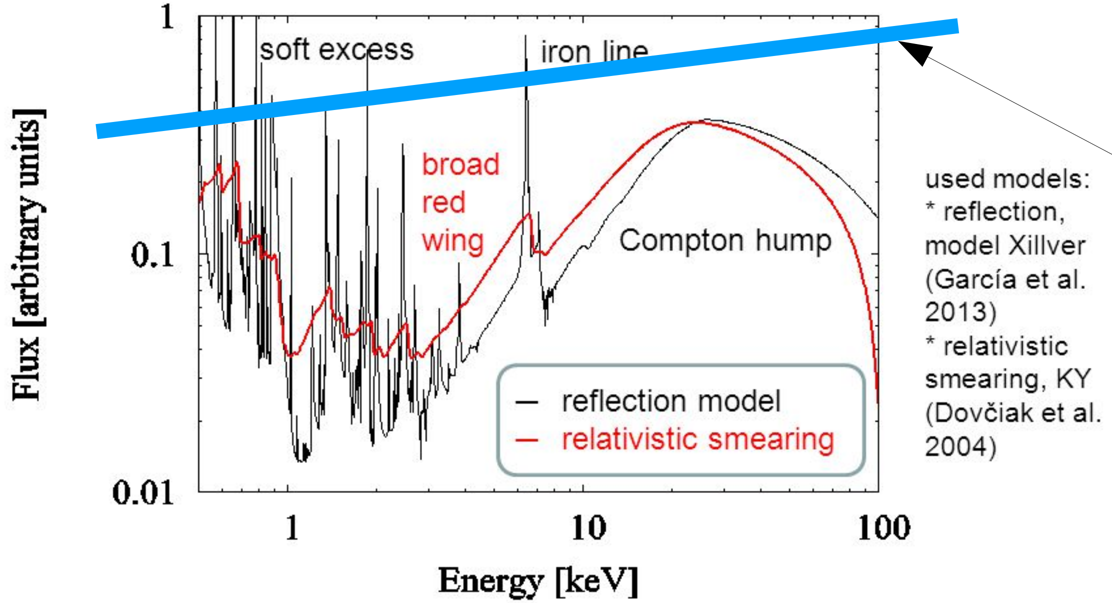

Incident power law continuum

Schematically:

Expected elastic reflection but

Strong absorption at low energies

Klein-Nishina decrease of the cross-section at high energies

10. Hot plasma temperature - heating/cooling

We did not talk about heating since, depending on geometry, we can postulate different mechanisms, or a combination of mechanisms

- Viscous heating (appropriate for hot inner flow)
- Magnetic heating (appropriate for a corona above the cold disk)
- Shocks and magnetic field reconnections (appropriate for highly turbulent flow)
- Extraction of black hole rotational energy (Blandford-Znajek, appropriate for jet ?)

Important aspect for thermal plasma: natural limit for the plasma temperature

As was shown many years ago (Bisnovatyi-Kogan in 70', Svensson in 80'), if the plasma is too hot and too compact, electron-position pairs will form in photon-photon collisions, and this will cool the plasma below ~ 500 keV

It is not yet clear if the cooling saturates due to pair production or just efficient Comptionization

(*From Fabian et al. 2015*)

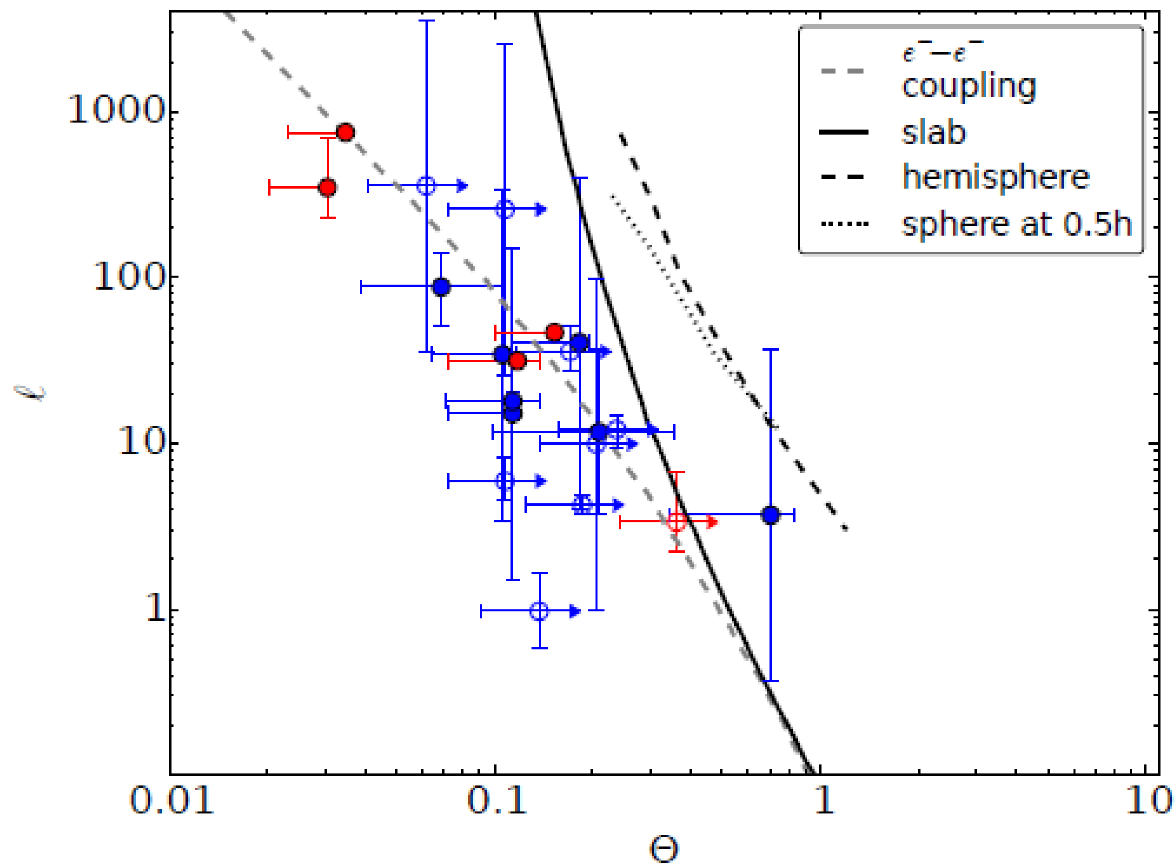

Figure 2. $\Theta - \ell$ distribution for *NuSTAR* observed AGN (blue points) and BHB (red points). The e–e coupling line from GHF is included. Pair lines from Stern et al (1995) are shown. The slab line has been extrapolated

Summary

- We know a lot about plasma cooling
- Plasma heating is less clear although we have a list of mechanisms (the same situation is in the solar corona)
- The geometry of the hot plasma is still under debate
- More problems to come
- No homework